Undulator radiation brightness calculations in the Sirepo GUI for SRW

B. Nash, O. Chubar, D. L. Bruhwiler, M. Rakitin, P. Moeller, et al.

B. Nash, O. Chubar, D. L. Bruhwiler, M. Rakitin, P. Moeller, R. Nagler, N. Goldring, "Undulator radiation brightness calculations in the Sirepo GUI for SRW," Proc. SPIE 11110, Advances in Laboratory-based X-Ray Sources, Optics, and Applications VII, 111100K (9 September 2019); doi: 10.1117/12.2530663

SPIE.

Event: SPIE Optical Engineering + Applications, 2019, San Diego, California, United States

Undulator radiation brightness calculations in the Sirepo GUI for SRW

B. Nash[a], O. Chubar[b], D. L. Bruhwiler[a], M. Rakitin[b], P. Moeller[a], R. Nagler[a], and N. Goldring[a]

[a]RadiaSoft LLC, Boulder, CO
[b]Brookhaven National Laboratory, Brookhaven, NY

ABSTRACT

The brightness and coherence of modern light sources is pushing the limits of X-ray beamline design. The open source Synchrotron Radiation Workshop (SRW) provides physical optics based algorithms for correctly simulating such beamlines.[1] We present new SRW capabilities to calculate source brightness and related quantites for undulators. The Sirepo cloud computing framework[2,3] includes a browser-based GUI for SRW.[4–6] In addition to high-accuracy wavefront simulations, the Sirepo interface now supports analytical calculations for flux, photon beam size, divergence and photon brightness. We have included the effects of detuning from resonance and electron beam energy spread, which can be important in realistic operational conditions. We compare our results to features previously available in the Igor Pro interface to SRW, to analytical formulae available in the literature, and also to the results of simulated wavefront propagation. Differences between the various approaches are explained in detail, so that all the assumptions, conventions and ranges of validity can be better understood.

Keywords: Synchrotron radiation, brightness, undulator, software

1. INTRODUCTION

In a recent SRI proceedings paper,[7] we presented a benchmarking between an analytical formula for flux, beamsize, divergence and brightness from an undulator, with wavefront computations using the SRW code. In this paper, we give further details for the analytical formulae and describe the implementation within the Sirepo framework. First, we specify the physical problem considered and give the definition of brightness in this context.

We consider the case of an electron beam passing through an elliptical undulator producing synchrotron radiation. In particular, we define the horizontal and vertical magnetic fields of the undulator to be

$$B_x = \begin{cases} B_{x0} \sin\left(\frac{2\pi s}{\lambda_u} + \phi_x\right) & |s| \le N\lambda_u/2 \\ 0 & |s| > N\lambda_u/2 \end{cases} \tag{1}$$

$$B_y = \begin{cases} B_{y0} \sin\left(\frac{2\pi s}{\lambda_u} + \phi_y\right) & |s| \le N\lambda_u/2 \\ 0 & |s| > N\lambda_u/2 \end{cases} \tag{2}$$

where $B_{x0,y0}$ are the maximal horizontal and vertical field strengths, λ_u is the undulator period length, $\phi_{x,y}$ are the magnetic field phases, N is the number of undulator periods, and s is the independent longitudinal coordinate along the undulator axis.

The electron beam passing through the undulator has a particular phase space distribution (typically Gaussian) which we denote as $f_e(\vec{z})$. The phase space coordinate $\vec{z}$ is given by

Further author information: (Send correspondence to B. Nash.)
E-mail: bnash@radiasoft.net

Advances in Laboratory-based X-Ray Sources, Optics, and Applications VII,
edited by Alex Murokh, Daniele Spiga, Proc. of SPIE Vol. 11110, 111100K
 · doi: 10.1117/12.2530663

$$\vec{z} = \begin{pmatrix} x \\ x' \\ y \\ y' \\ z \\ \delta \end{pmatrix} = \begin{pmatrix} \vec{z}_\perp \\ z \\ \delta \end{pmatrix} \tag{3}$$

where x, y, z represent the horizontal, vertical and longitudinal coordinates respectively, x' and y' are the horizontal and vertical divergences, and δ is defined as $\frac{E-E_0}{E_0}$ where E_0 is the electron beam reference energy. We have divided up the phase space in to transverse ($\vec{z}_\perp$) and longitudinal (z, δ) components. It is often the case that one can approximately factorize the phase space distribution as $f(\vec{z}) = f_\perp(\vec{z}_\perp) f_l(z, \delta)$. We note, however, that dispersion will invalidate this relation.

The RMS electron beam sizes, $\sigma_{x,y,eb}$, divergences, $\sigma_{x',y',eb}$, and energy spread, σ_δ, are defined from the electron beam distribution as follows.

$$\sigma^2_{x,eb} = \left\langle x^2 \right\rangle_{f_e} \tag{4}$$
$$\sigma^2_{y,eb} = \left\langle y^2 \right\rangle_{f_e} \tag{5}$$
$$\sigma^2_{x',eb} = \left\langle x'^2 \right\rangle_{f_e} \tag{6}$$
$$\sigma^2_{y',eb} = \left\langle y'^2 \right\rangle_{f_e} \tag{7}$$
$$\sigma^2_{\delta} = \left\langle \delta^2 \right\rangle_{f_e} \tag{8}$$

where the subscript f_e denotes averaging over the electron beam distribution.

Now, this electron beam will emit synchrotron radiation as it passes through the undulator. Let $\Phi_{r,1}(\vec{r}, \omega, \vec{z}, s)$ be the flux density at frequency ω computed in a plane a distance s from the center of the undulator due to a single electron. The electron is at phase space position $\vec{z}$ relative to the center of the undulator ($s = 0$). One may also define the single-electron flux density in the angular representation, $\Phi_{\theta,1}(\vec{\theta}, \omega, \vec{z}, s)$, which may be computed from $\Phi_{r,1}(\vec{r}, \omega, \vec{z}, s)$ by Fourier transform.

At this point, we introduce the effect of energy spread by averaging the single electron flux, $\Phi_{r,1}(\vec{r}, \omega, \vec{z}, s)$, over the longitudinal electron phase space. In particular, we define

$$\Phi_{r,1,es}(\vec{r}, \omega, \vec{z}_\perp, s) = \frac{1}{\sqrt{2\pi}\sigma_\delta} \int_{-\infty}^{\infty} \Phi_{r,1}(\vec{r}, \omega, \vec{z}, s) e^{-\frac{\delta^2}{2\sigma^2_\delta}} d\delta \tag{9}$$

From now, we drop the es subscript, noting the dependence on $\vec{z}_\perp$ rather than $\vec{z}$. Due to the incoherence of synchrotron radiation, we may neglect the longitudinal coordinate , z, in what follows.

The photon beam size, $\sigma_{r,pb}$, and divergence, $\sigma_{r',pb}$, are defined as*

$$\sigma^2_{r,pb} = \frac{1}{\Phi_1} \int r^2 \Phi_{r,1}(\vec{r}, \omega, \vec{z}_\perp, s) d\vec{r} \tag{10}$$
$$\sigma^2_{r',pb} = \frac{1}{\Phi_1} \int \theta^2 \Phi_{\theta,1}(\vec{\theta}, \omega, \vec{z}_\perp, s) d\vec{\theta} \tag{11}$$

where Φ_1 is the total single-electron flux defined as

$$\Phi_1 = \int \Phi_{r,1}(\vec{r}, \omega, \vec{z}, s) d\vec{r} = \int \Phi_{\theta,1}(\vec{\theta}, \omega, \vec{z}, s) d\vec{\theta} \tag{12}$$

*We assume that there is a symmetry in the radiation which, in fact, is only approximate due to an asymmetry in the electron orbit.

For the total multi-electron flux density, we integrate the single-electron flux density over the electron beam distribution for all phase space positions, $\vec{z}$:

$$\Phi_r(\vec{r},\omega,s) = \int \Phi_{r,1}(\vec{r},\omega,\vec{z},s) f_e(\vec{z}) d\vec{z} \tag{13}$$

The total multi-electron flux is given by

$$\Phi(\omega) = \int \Phi_r(\vec{r},\omega,s) d\vec{r} = \int \Phi_\theta(\vec{\theta},\omega,s) d\vec{\theta} \tag{14}$$

where the integration is over the entire plane of observation. The multi-electron angular distribution, Φ_θ, is defined from $\Phi_{\theta,1}$ in the same way as Φ_r is defined from $\Phi_{r,1}$. We also note that the total flux is independent of the distance to the plane of observation, s.

We can now define the photon beam sizes, $\Sigma_{x,y}$, and divergences, $\Sigma_{x',y'}$, for the multi-electron flux density distribution as follows.

$$\Sigma_x^2 = \frac{1}{\Phi} \int r_x^2 \Phi_r(\vec{r},\omega,s) d\vec{r} \tag{15}$$

$$\Sigma_y^2 = \frac{1}{\Phi} \int r_y^2 \Phi_r(\vec{r},\omega,s) d\vec{r} \tag{16}$$

$$\Sigma_{x'}^2 = \frac{1}{\Phi} \int \theta_{x'}^2 \Phi_\theta(\vec{\theta},\omega,s) d\vec{\theta} \tag{17}$$

$$\Sigma_{y'}^2 = \frac{1}{\Phi} \int \theta_{y'}^2 \Phi_\theta(\vec{\theta},\omega,s) d\vec{\theta} \tag{18}$$

A common situation with undulators without substantial errors and relatively simple beamline elements results in the validity of the brightness convolution theorem.[8] In this case, the photon flux density produced by an electron offset by $\vec{z}_\perp$ can be approximated as being shifted from the flux density produced by an electron at the origin of the electron bunch ($\vec{z}_\perp = \vec{0}$). The translated photon flux density may be written as

$$\Phi_{r,1}(\vec{r},\omega,\vec{z},s) = \Phi_{r,1}(\vec{r} - M\vec{z}_\perp,\omega,\vec{0},s) \tag{19}$$

where $M\vec{z}_\perp$ is a linear transformation of the electron through free space from the center of the undulator to the plane of observation. Upon applying Eqn. (19), one finds that Eqn. (13) becomes a simple convolution.

Under the conditions in which the convolution theorem holds and approximating the photon flux density as Gaussian, one may find the photon beam sizes for the multi-particle radiated flux density by adding electron and photon beam sizes in quadrature and likewise for the divergences.

$$\Sigma_{x,y}^2 = \sigma_{x,y,eb}^2 + \sigma_{r,pb}^2 \tag{20}$$

$$\Sigma_{x',y'}^2 = \sigma_{x',y',eb}^2 + \sigma_{r',pb}^2 \tag{21}$$

We may express the horizontal and vertical emittances for the full photon beam as follows.

$$\varepsilon_{x,y} = \Sigma_{x,y}\Sigma_{x',y'} - \Sigma_{xx',yy'}^2 \tag{22}$$

Finally, we may describe the brightness of the undulator source in terms of the photon beam emittances and total flux. Formally, the brightness of a synchrotron radiation source is defined as the central value of the multi-electron Wigner function for the radiation,[9] normalized by the total flux. However, in the case of nearly Gaussian Wigner function, one may approximate the brightness with the following formula.

$$B = \frac{\Phi(\omega)}{4\pi^2 \varepsilon_x \varepsilon_y} \tag{23}$$

In further sections, we give expressions for the flux and single-electron beam sizes and divergences accounting for elliptical undulators, electron beam energy spread, and photon energy detuning from resonance. The expressions were previously presented[7] using so-called universal functions. Here, we will give explicit forms for these functions including some detail on their derivation.

2. DERIVATION OF PHOTON BEAM FLUX

In this section, we sketch a derivation for the flux density passing through an undulator as described above. This derivation is based on unpublished notes by Oleg Chubar. The reader may also refer to the paper by Tanaka and Kitamura[10] which we generalize to include elliptical undulators and the effects of photon energy detuning from resonance.

The flux density per unit frequency for a single electron emitting undulator radiation and including the effects of energy spread is given by

$$\Phi_{r,1}(\vec{r}, \omega, \vec{z}_\perp, s) = \frac{dN_{ph}}{dt(d\omega/\omega)d\vec{r}} = \frac{c^2 \alpha I_b}{4\pi^2 e^3} \int_{-\infty}^{\infty} \left| \vec{E}_{\omega 1}(\vec{r}; \vec{z}, s) \right|^2 \frac{e^{-\frac{\delta^2}{2\sigma_\delta^2}}}{\sqrt{2\pi}\sigma_\delta} d\delta \tag{24}$$

where c is the speed of light in vacuum, α is the fine structure constant, I_b is the electron beam current, and e is the elementary charge. $\vec{E}_{\omega 1}(\vec{r}; \vec{z})$ is the radiated electric field at a fixed frequency ω resulting from a single electron at phase space position $\vec{z}$.

The radiated electric field is given by

$$\vec{E}_{\omega 1}(\vec{r}; \vec{z}) = \frac{ie\omega}{4\pi\varepsilon_0 c} \int_{-\infty}^{\infty} \frac{1}{R(\tau)} \left[\vec{\beta}(\tau) - \left(1 + \frac{ic}{\omega R(\tau)} \right) \hat{n} \right] e^{[i\omega(\tau + R/c)]} d\tau \tag{25}$$

with ε_0 the dielectric constant (SI units), $\vec{\beta}(\tau)$ the transverse electron velocity normalized by c, $\vec{R}$ the vector between the electron position and the position of observation, and $\hat{n}$ a unit vector in the direction of $\vec{R}$.

In the far-field, where $|\vec{z}|, |\vec{r}| \ll \left|\vec{R}\right|$, we may take the vector $\vec{R}$ out of the integral in Eqn. (25) and drop the $1/\vec{R}$ term yielding

$$\vec{E}_{\omega 1}(\vec{r}; \vec{z}) \approx \frac{ie\omega}{4\pi\varepsilon_0 c} \frac{1}{R_0} \int_{-\infty}^{\infty} \left(\vec{\beta}(s) - \hat{n} \right) e^{[i\omega(\tau(s) + R/c)]} ds \tag{26}$$

Making a small angle approximation, one may write

$$\hat{n} = \left(\theta_x, \theta_y, 1 - \theta^2/2 \right) \tag{27}$$

where θ is the angle of observation defined as $\theta^2 = \theta_x^2 + \theta_y^2$.

The argument in the exponent in Eqn. (26) may be written as

$$\tau + R/c = \frac{1}{2c} \left[\frac{s}{\gamma^2} + \int_0^s \left[(\beta_x - \theta_x)^2 + (\beta_y - \theta_y)^2 \right] ds + \theta^2 Z \right] \tag{28}$$

where Z is the distance between the center of the undulator and the origin of the plane of observation.

The integration over the full undulator can now be broken down into a summation over integrals over individual undulator periods as follows.

$$\vec{E}_{\omega 1}(\vec{r};\vec{z}) \approx \frac{ie\omega}{4\pi\varepsilon_0 c}\frac{1}{R_0}N\sum_n f_n(\gamma,\theta_x,\theta_y)\,\mathrm{sinc}\left[n\pi N\frac{\omega-\omega_n}{\omega_n}\right]e^{i\omega\frac{\theta^2 Z}{2c}} \tag{29}$$

where ω_n denotes the nth resonant frequency.

The quantity $f_n(\gamma,\theta_x,\theta_y)$ is calculated by

$$f_n(\gamma,\theta_x,\theta_y) = \frac{i\omega_n}{cR_0}\int_0^{\lambda_u}\left[\vec{\beta}(s)-\hat{n}\right]e^{\frac{i\omega_n}{2c}\left[\frac{s}{\gamma^2}+\int_0^s\left[(\beta_x-\theta_x)^2+(\beta_y-\theta_y)^2\right]ds\right]}ds \tag{30}$$

We now consider a non-planar undulator with both horizontal and vertical magnetic fields. An electron passing through the magnetic fields described by Eqn.'s (1) and (2) will be bent sinusoidally and one may derive the following expressions for its velocity along the undulator.

$$\beta_x = \begin{cases}\frac{k_x}{\gamma}\cos\left(\frac{2\pi s}{\lambda_u}+\phi_x\right) & |s|\le N\lambda_u/2\\ 0 & |s|>N\lambda_u/2\end{cases} \tag{31}$$

$$\beta_y = \begin{cases}-\frac{k_y}{\gamma}\cos\left(\frac{2\pi s}{\lambda_u}+\phi_y\right) & |s|\le N\lambda_u/2\\ 0 & |s|>N\lambda_u/2\end{cases} \tag{32}$$

The undulator parameters, k_x and k_y are given by

$$k_x = \frac{eB_{y0}\lambda_u}{2\pi m_e c} \tag{33}$$

$$k_y = \frac{eB_{x0}\lambda_u}{2\pi m_e c} \tag{34}$$

The relativistic factor, γ, is given from the electron energy by

$$\gamma = \frac{E_0}{m_e c} \tag{35}$$

where m_e is the electron mass.

The resonant frequency for a general elliptical undulator is given by

$$\omega_n = \frac{n\gamma^2}{\lambda_u}\frac{4\pi c}{1+K^2/2+\gamma^2\theta^2} \tag{36}$$

with $K^2 = k_x^2 + k_y^2$.

Next, we define hybrid undulator parameters which will prove convenient to express our final results.

$$k_1^2 = k_y^2\cos^2(\phi_x-\phi_0) + k_x^2\cos^2(\phi_y-\phi_0) \tag{37}$$

$$k_2^2 = k_y^2\sin^2(\phi_x-\phi_0) + k_x^2\sin^2(\phi_y-\phi_0) \tag{38}$$

$$\phi_0 = \frac{1}{2}\tan^{-1}\left(\frac{k_y^2\sin 2\phi_x + k_x^2\sin 2\phi_y}{k_y^2\cos 2\phi_x + k_x^2\cos 2\phi_y}\right) \tag{39}$$

$$qq = \frac{n}{4}\frac{k_1^2-k_2^2}{1+\frac{1}{2}(k_1^2+k_2^2)} \tag{40}$$

We also define a normalized energy spread and detuning factor given by Δ and ϵ respectively.

$$\epsilon = Nn\sigma_\delta \tag{41}$$

$$\Delta = Nn\frac{\omega - \omega_n}{\omega_n} \tag{42}$$

Now that we have an expression for $\vec{E}_{\omega 1}(\vec{r};\vec{z})$, we substitute it in to Eqn. (24) and do the integral over the electron phase space. Finally, we integrate over the plane of observation using Eqn. (14) and neglecting some of the details, we arrive at our expression for the total flux.

$$\Phi = C_0 N I_b \frac{nk_1^2}{1+\frac{K^2}{2}} \overline{JJ}^2(qq) F_f(\Delta,\epsilon) G(\Delta,k_1,k_2) \tag{43}$$

where we define $\overline{JJ}^2(qq)$ as a generalization of the standard Bessel function factor, JJ:

$$\overline{JJ}^2(qq) = \left[J_{\frac{n-1}{2}}(qq) - J_{\frac{n+1}{2}}(qq)\right]^2 + \frac{k_2^2}{k_1^2}\left[J_{\frac{n-1}{2}}(qq) + J_{\frac{n+1}{2}}(qq)\right]^2 \tag{44}$$

The constant C_0 is defined as

$$C_0 = \frac{\alpha d\omega/\omega}{e} = 4.5546497 \times 10^{13}\text{Coulombs}^{-1} \tag{45}$$

where $d\omega/\omega$ is the frequency bandwidth and, as is conventionally done, is set to 0.01%. The factor G is an additional correction factor, higher order in the energy deviation.

$$G = \frac{1}{2}(1+e^{\frac{a_\sigma^2}{2}})(1-\mathbf{erf}(\frac{a_\sigma}{\sqrt{2}})) \tag{46}$$

$$a_\sigma = 2m_a\frac{dE}{E}, \qquad m_a = \frac{n^2(k_1^2+k_2^2)}{w_f^2(1+\frac{1}{2}(k_1^2+k_2^2))} \tag{47}$$

where w_f is a fitting parameter equal to 0.63276.

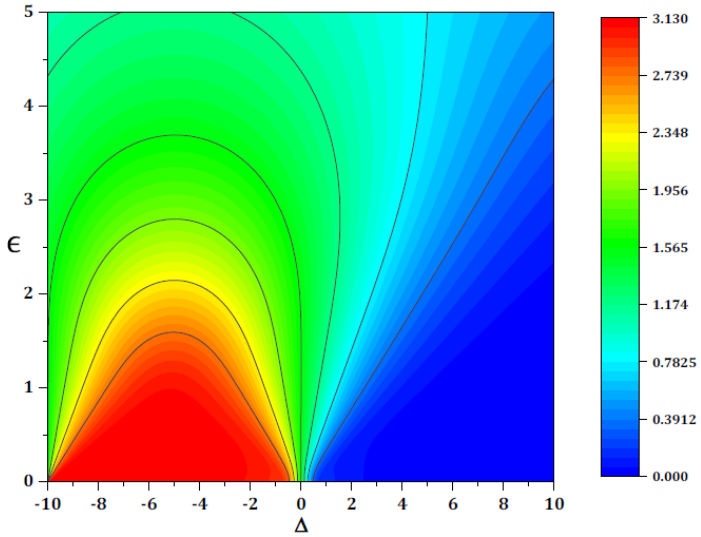

Figure 1: Universal function for photon flux, F_f. This contour plots provide the effect of energy spread and detuning from resonance on these quantities.

To derive the universal function for photon beam flux, we return to Eqn. (29). Near one of the resonances, only one of the terms in the sum will survive. Further, in the case of exactly on resonance and without energy deviation, the sinc function will go to zero. The correction factor simply comes from allowing the photon energy to be off resonance and the single electron energy to be away from its nominal value. Expanding the sinc function in terms of these small deviations, one finds the correction factor given by

$$F_{1,far}(\Delta, t, \Theta) = \text{sinc}\left[\pi(\Delta - 2t) + \Theta^2\right] \tag{48}$$

where

$$\Theta = \gamma_0 \theta \left(\frac{\pi N n}{1 + K^2/2}\right)^{1/2} \tag{49}$$

$$t = nN\delta \tag{50}$$

and the subscript far refers to the fact that we have computed the electric field in the far-field.

Following from Eqn. (24), we now include energy spread by integrating with respect to t:

$$P_{far}(\Delta, \epsilon, \Theta) = \frac{1}{\sqrt{2\pi}\epsilon} \int_{-\infty}^{\infty} F_{1,far}^2(\Delta, t, \Theta) e^{-\frac{t^2}{2\epsilon^2}} dt \tag{51}$$

Now, given $P_{far}(\Delta, \epsilon, \Theta)$, we integrate over Θ to get the universal function for flux:

$$F_f(\Delta, \epsilon) = 2 \int_0^{\infty} P_{far}(\Delta, \epsilon, \Theta) \Theta d\Theta \tag{52}$$

The paper by Tanaka and Kitamura did not consider the effect of spectral detuning. Turning this effect off means settings $\Delta = 0$. In this case, we find that Eqn. (51) reduces to Eqn. (12) in Tanaka.

After substituting in all relevant expressions, we find an explicit definition for the universal function for undulator flux.

$$F_f(\Delta, \epsilon) = \frac{2}{\sqrt{2\pi}\epsilon} \int_0^{\infty} \int_{-\infty}^{\infty} \theta \, \text{sinc}^2\left[\pi\left(\Delta - 2t\right) + \Theta^2\right] e^{-t^2/2\epsilon^2} dt d\theta \tag{53}$$

The above function was calculated numerically within Igor Pro and is plotted in Fig. [1].

3. PHOTON BEAM SIZE AND DIVERGENCE

To compute the photon beam size and divergence from a single electron, we use Eqn.'s (10) and (11). Given the computation of the electric field in the previous section, we can compute these. Note in particular that in Eqn. (24), the energy spread has been included. We want to calculate beam sizes and divergences on-axis and so we set $\vec{z}_\perp$ equal to zero. Expressions for RMS photon beam size and divergence values are given as in the text by Onuki and Elleaume,[11] but with additional correction for energy spread and detuning via universal functions F_r and $F_{r'}$:

$$\sigma_{r,pb} = \frac{1}{2}\sqrt{\lambda_n L} \; F_r(\Delta, \epsilon) \tag{54}$$

$$\sigma_{r',pb} = \sqrt{\frac{\lambda_n}{L}} \; F_{r'}(\Delta, \epsilon) \tag{55}$$

where L is the undulator length and λ_n is the on-resonance spectral wavelength of the nth harmonic defined as

$$\lambda_n = \frac{\lambda_u}{2n\gamma^2}\left(1 + \frac{K^2}{2}\right) = \frac{2\pi}{\omega_n(\theta = 0)} \tag{56}$$

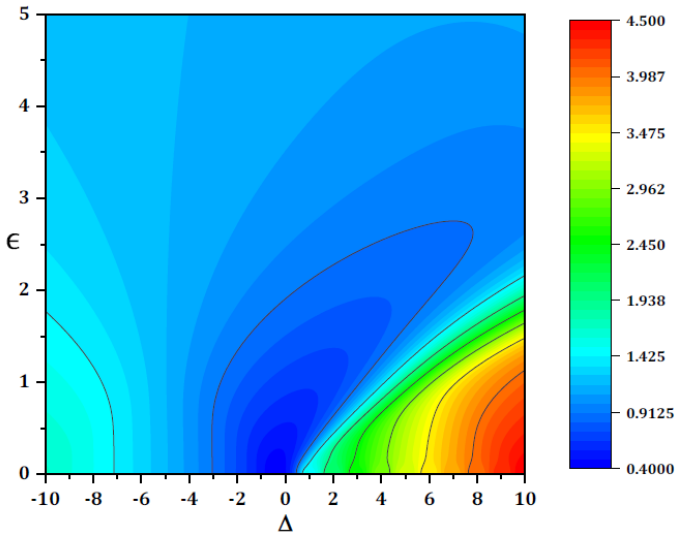

(a) Beam size correction

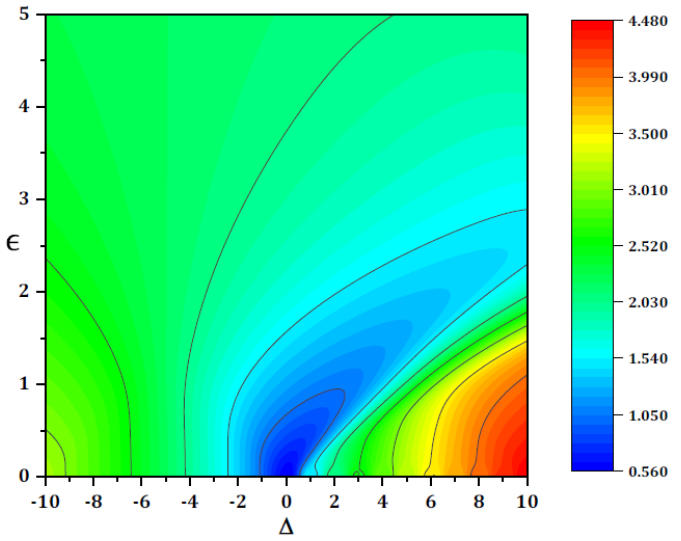

(b) Beam divergence correction

Figure 2: Universal functions for beam size, F_r and divergence, $F_{r'}$. These contour plots provide the effect of energy spread and detuning from resonance on these quantities.

As with the universal function for photon beam flux, the universal functions for photon beam size and divergence were calculated over a range of energy deviations and detuning values via Igor Pro and plotted in Fig. [2]. We note that $F_r(0,0) = 0.4717$ and $F_{r'}(0,0) = 0.5795$.

The universal function for undulator RMS angular divergence can be expressed as

$$F_{r'}(\Delta, \epsilon, m) = \left[\frac{2\pi}{F_f(\Delta, \epsilon)} \int_0^{\Theta_m} P_{far}(\Delta, \epsilon, \Theta) \Theta^3 d\Theta \right]^{1/2} \tag{57}$$

where m describes the amount of flux included in the calculation. We note that integrating to infinity would give a divergence and thus a maximum angle cutoff is required. Typically, one uses a value of m between 0.95 and 0.99 and the maximum angle is defined implicitly in the following relation.

$$\frac{2\pi}{F_f(\Delta,\epsilon)}\int_0^{\Theta_m} P_{far}(\Delta,\epsilon,\Theta)d\Theta = 1 \tag{58}$$

The universal function for RMS beam size can be expressed as

$$F_r(\Delta,\epsilon,m) = \left[\frac{2\pi}{F_f(\Delta,\epsilon)}\int_0^{\rho_m} P_{near}(\Delta,\epsilon,\rho)\rho^3 d\rho\right]^{1/2} \tag{59}$$

Similarly to the expression for divergence, the maximum position to integrate over is defined implicitly by

$$\frac{2\pi}{F_f(\Delta,\epsilon)}\int_0^{\rho_m} P_{near}(\Delta,\epsilon,\rho)d\rho = 1 \tag{60}$$

$P_{near}(\Delta,\epsilon,\rho)$ is defined as

$$P_{near}(\Delta,\epsilon,\rho) = \frac{1}{\sqrt{2\pi\epsilon}}\int_{-\infty}^{\infty} |F_{1,near}(\Delta-2t,\rho)|^2\, e^{-\frac{t^2}{2\epsilon}} dt \tag{61}$$

where $F_{1,near}$ can be expressed in terms of $F_{1,far}$ as follows.

$$F_{1,near}(\Delta,\Theta) = \int_{-\infty}^{\infty}\int_{-\infty}^{\infty} F_{1,far}\left(\Delta,\sqrt{\Theta_x^2+\Theta_y^2}\right) e^{2\pi i(\Theta_x x+\Theta_y y)} d\Theta_x\Theta_y \tag{62}$$

4. IMPLEMENTATION IN THE SIREPO FRAMEWORK

The analytic expressions and numerical correction factors for flux, size, and divergence presented above have been implemented in a Python library[12] and are available within the Sirepo interface to SRW in the brightness report. The brightness report uses the electron beam and undulator parameters defined on the source page and are used for all other SRW simulations. The Sirepo brightness report may be used in two basic modes. One is called K-tuning and the other is called spectral detuning.

In the K-tuning simulation, we consider varying the undulator gap and computing various quantities for a photon energy at a fixed distance from each particular undulator resonance. The K-tuning brightness curves are the standard metric used to evaluate the performance of a synchrotron light source with a given undulator. They indicate ranges of energy that will optimize the available photons for different experiments.

In the spectral detuning simulation, the gap of the undulator is fixed and one varies the observed energy of the photon beam away from the resonant value. The spectral detuning curves provide insight into how one may tune an undulator to maximize the flux or to fine tune the properties of the beam. We observe, for example, that detuning an undulator provides at least a factor of two increase in photon flux. One can also study the variation in the photon beam size and divergences which are important in their own rights but also have an impact on the resulting brightness. The K-tuning analysis may be performed for different detuning values which may be of interest, for example, to explore the performance of an undulator detuned to maximize flux.

The results displayed in Fig. [4,5,6,7] were obtained from simulations for the NSLS-II Low Beta electron beam, the parameters of which are displayed in Fig. [3a]. We also simulate an elliptical undulator, the parameters of which are shown in Fig. [3b]. The resonant energy of the first, third, and fifth harmonics are 411.59 eV, 1234.8 eV, and 2057.9 eV respectively.

Fig. [4] shows the electron trajectory passing through the undulator that has been defined. Fig. [5] shows a series of radiation calculation results from this electron beam and undulator. In Fig. [5a], the peak at the first resonant energy is displayed. In [5b], we see a broader range of photon energies so that multiple peaks are visible. This report includes the effects of emittance and energy spread for radiation passing through a finite aperture. Note that the even harmonics, which are forbidden in the single electron case with an infinitesimal aperture, are visible in this calculation though strongly suppressed. Finally, Fig. [5c,d] display the intensity and power density which includes an integration over all energies.

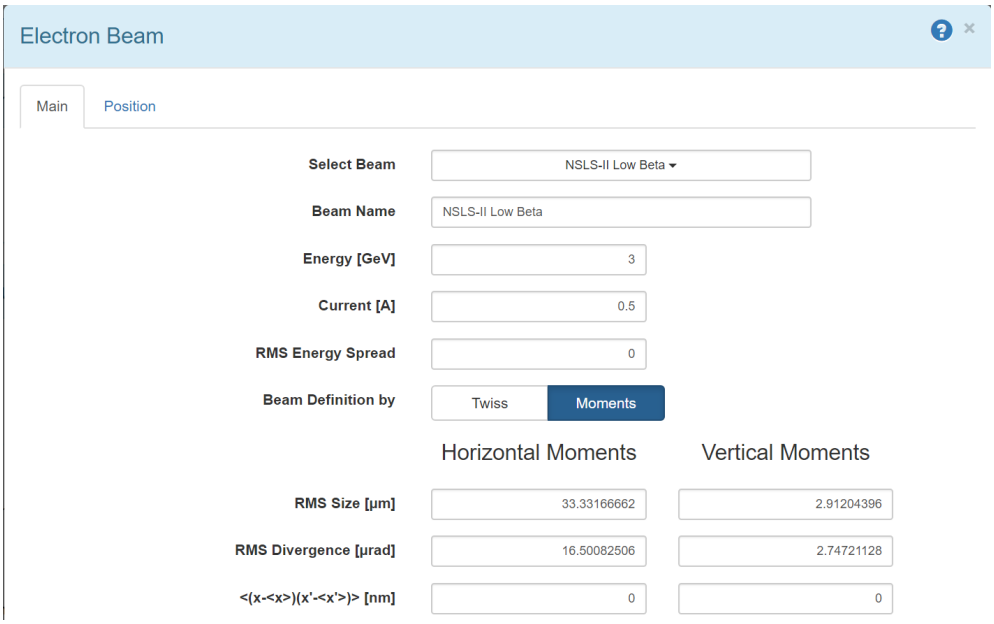

(a) Electron beam input parameters

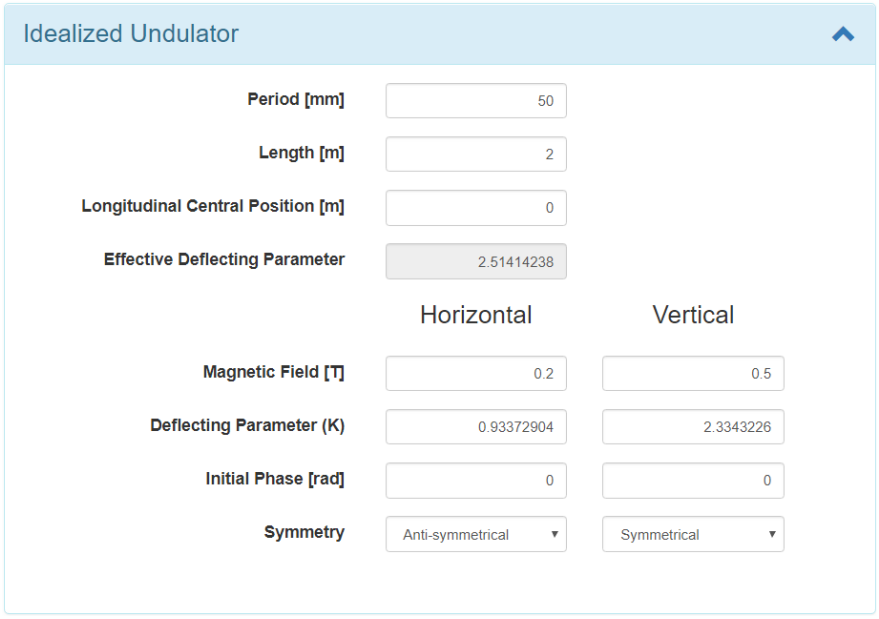

(b) Undulator input parameters

Figure 3: Screenshot of parameter input windows within the Sirepo SRW interface. Electron beam parameters represent the NSLS-II Low Beta beam and undulator parameters reflect an arbitrary ellipsoidal undulator.

To emphasize the effect of energy spread, we consider the same undulator described above, but with double the length (L = 4 m, N = 80 periods). Furthermore, we consider the n=15 harmonic. We use an energy spread of $\sigma_\delta = 10^{-3}$ which leads to a normalized energy spread parameter of $\epsilon = 1.5$. The energy of the 15^{th} harmonic is 6173.8 eV and we have detuned to below the resonance by 5 eV which gives a normalized detuning parameter of $\Delta = -1$. The results of the flux calculations with and without energy spread are shown in Fig. [8]. We note that the energy spread has resulted in a 50% decrease in flux.

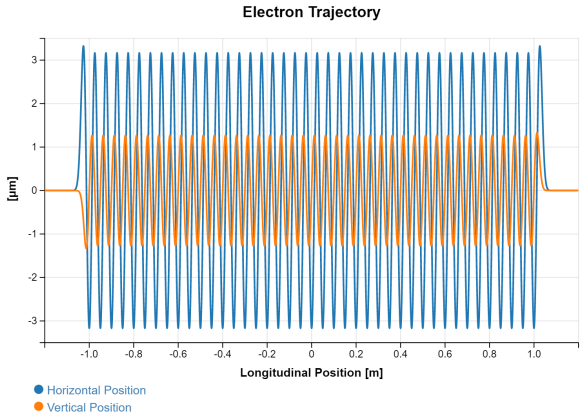

Figure 4: Screenshot of electron beam horizontal and vertical trajectory for ellipsoidal undulator showing helical orbit.

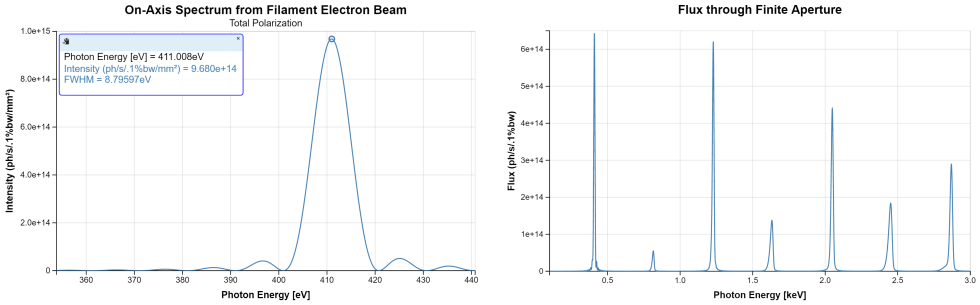

(a) Single-electron spectrum report (b) Multi-electron spectrum report

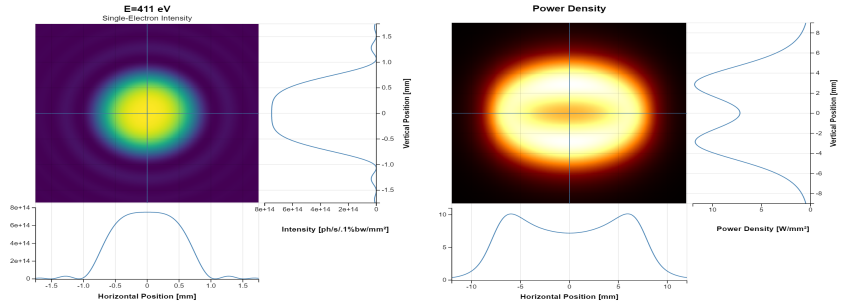

(c) Spectral flux report (d) Power density report

Figure 5: Sirepo display of SRW calculation results for elliptical undulator and electron beam with parameters defined in previous figures.

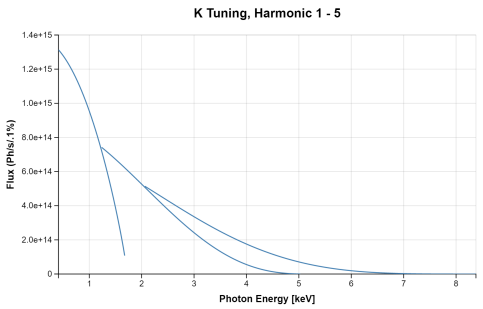

(a) Flux

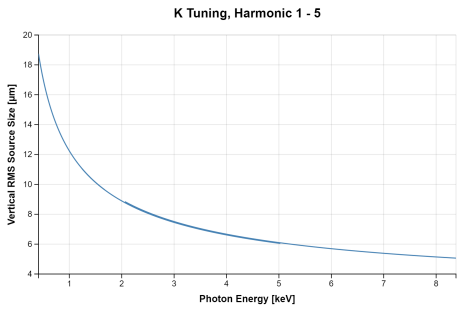

(b) RMS size

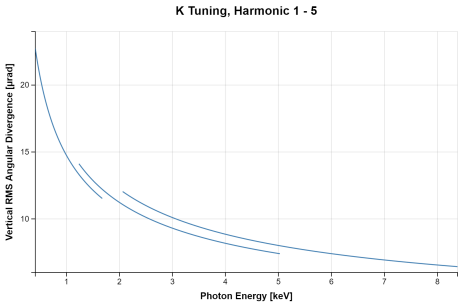

(c) RMS divergence

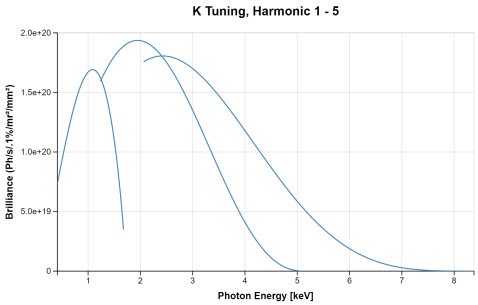

(d) Brightness

Figure 6: K-tuning plots for various quantities generated in Sirepo/SRW with the brightness Python library.

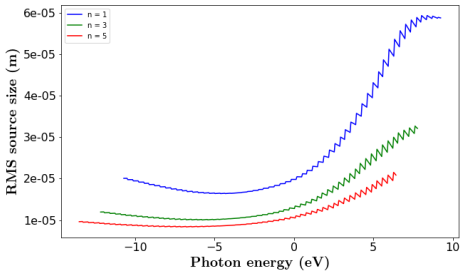

(a) RMS beam size

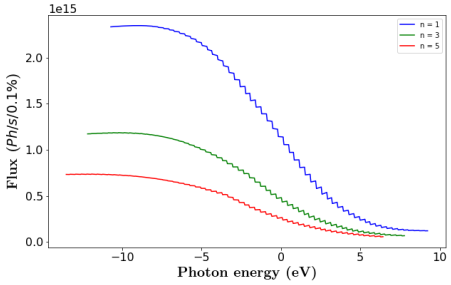

(b) Flux

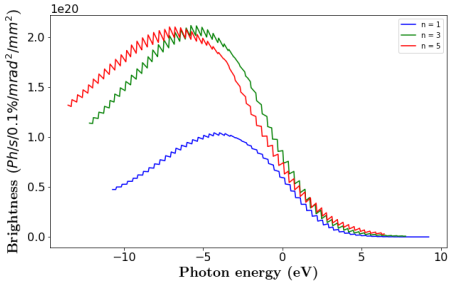

(c) Brightness

Figure 7: Spectral detuning plots for photon beam RMS size, flux, and brightness for n = 1,3, and 5. The data in was extracted from the brightness reports in the Sirepo/SRW interface and further processed to create these plots.

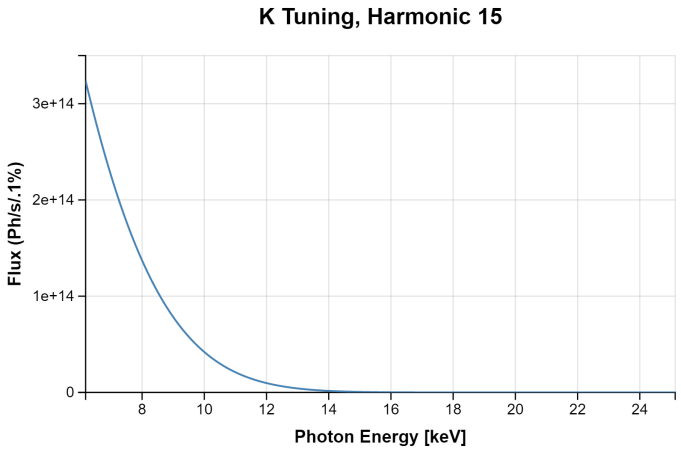

(a) Without energy spread

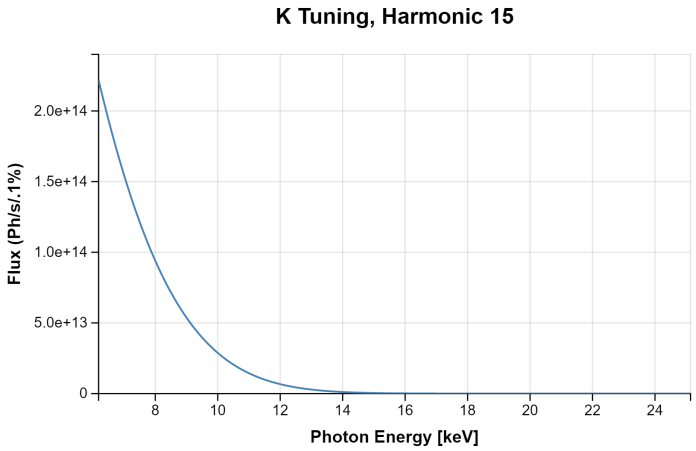

(b) With energy spread

Figure 8: n=15 K-tuning flux plots produced by Sirepo/SRW.

5. CONCLUSION

In this paper, we have expanded upon our previous work in which we benchmarked the formulae for flux, brightness, photon beam sizes and divergences versus SRW calculations. Those formulae, previously available only in the Igor Pro interface to SRW are now available in the Sirepo cloud computing interface. All of these quantities have dependence on energy spread and detuning from resonance which is captured in a numerically computed universal function. Here, we have given explicit expressions for the universal functions, and shown how the flux correction factor reduces to the results of Tanaka and Kitimura when the spectral detuning is ignored. We have also described how the results of Tanaka and Kitimura are generalized to include elliptical undulators.

We have given examples of the uses of the brightness library in Sirepo, which has been integrated and is available via a report on the source page in Sirepo/SRW. In particular, we showed an example of an elliptically polarized undulator, displayed the spectral flux and power density as well as the electron trajectories. We examined both the K-tuning and spectral detuning curves for this example, the K-tuning representing the opening of the undulator gap and the subsequent change in beam properties for the various odd harmonics. The spectral detuning represents the variation of the beam parameters for a fixed undulator gap, but varying photon energy. We plotted the beam properties for the elliptical undulator for several harmonics by downloading the data produced by Sirepo, further showing the flexibility provided by this web browser based interface to SRW. Finally, we gave an example where energy spread decreased the flux of an n=15 undulator harmonic by 50%. This result showed that energy spread can indeed produce an important degradation of performance in third generation undulator-based light sources. Having a convenient tool to assess this impact can aid in the design process for future light sources as well as for upgrades of existing facilities.

ACKNOWLEDGMENTS

This material is based upon work supported by the U.S. Department of Energy, Office of Science, Office of Basic Energy Sciences, under Award Numbers DE-SC0011237 and DE-SC0018571.

REFERENCES

[1] Chubar, O. and Elleaume, P., "Accurate and efficient computation of synchrotron radiation in the near field region," *Proc. of EPAC-98* , 1177–1179 (1998).

[2] Rakitin, M. S., Moeller, P., Nagler, R., Nash, B., Bruhwiler, D. L., Smalyuk, D., Zhernenkov, M., and Chubar, O., "*Sirepo*: an open-source cloud-based software interface for X-ray source and optics simulations," *Journal of Synchrotron Radiation* **25**, 1877–1892 (Nov 2018).

[3] "The sirepo source code repository." https://github.com/radiasoft/sirepo.

[4] "The public sirepo/srw server." https://sirepo.com/#/srw.

[5] Rakitin, M., Chubar, O., Moeller, P., Nagler, R., and Bruhwiler, D. *Proc. Adv. Comp. Meth. X-Ray Optics IV* (2017).

[6] Rakitin, M. S., Moeller, P., Nagler, R., Nash, B., Bruhwiler, D. L., Smalyuk, D., Zhernenkov, M., and Chubar, O., "*Sirepo*: an open-source cloud-based software interface for X-ray source and optics simulations," *Journal of Synchrotron Radiation* **25**, 1877–1892 (Nov 2018).

[7] Nash, B., Chubar, O., Goldring, N., Bruhwiler, D. L., Moeller, P., Nagler, R., and Rakitin, M., "Detailed x-ray brightness calculations in the sirepo gui for srw," *AIP Conference Proceedings* **2054**(1), 060080 (2019).

[8] Kim, K.-J., "A new formulation of synchrotron radiation optics using the wigner distribution," (1986).

[9] Kim, K.-J., "Brightness, coherence and propagation characteristics of synchrotron radiation," *Nuclear Instruments and Methods in Physics Research Section A: Accelerators, Spectrometers, Detectors and Associated Equipment* **246**(1), 71 – 76 (1986).

[10] Tanaka, T. and Kitamura, H., "Universal function for the brilliance of undulator radiation considering the energy spread effect," *Journal of Synchrotron Radiation* **16**, 380–386 (2009).

[11] Onuki, H. and Elleaume, P., [*Undulators, Wigglers and their Applications*], CRC Press (2002).

[12] "Sirepo srw brightness function library." https://github.com/radiasoft/sirepo/blob/master/sirepo/template/srwl_uti_brightness.py.